

Optical bistability in shape-memory nanowire metamaterial array

Yusuke Nagasaki, Behrad Gholipour, Jun-Yu Ou, Masanori Tsuruta, Eric Plum, Kevin F. MacDonald, Junichi Takahara, and Nikolay I. Zheludev

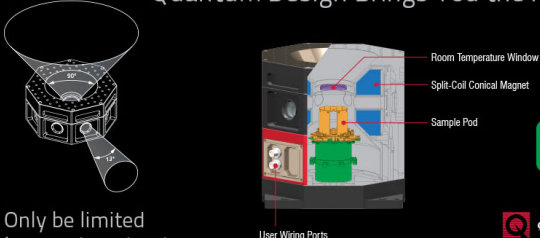
Citation: *Appl. Phys. Lett.* **113**, 021105 (2018); doi: 10.1063/1.5025400

View online: <https://doi.org/10.1063/1.5025400>

View Table of Contents: <http://aip.scitation.org/toc/apl/113/2>

Published by the [American Institute of Physics](#)

Quantum Design Brings You the Next Generation Magneto-Optic Cryostat



Only be limited by your imagination...

[Learn More](#)

8 Optical Access Ports: 7 Side; 1 Top
Temperature Range: 1.7 K to 350 K
7 T Split-Coil Conical Magnet
Low Vibration: <10 nm peak-to-peak
89 mm x 84 mm Sample Volume
Automated Temperature & Magnet Control
Cryogen Free

 **OptiCool**

 **Quantum Design**
qdusa.com/opticool5

Optical bistability in shape-memory nanowire metamaterial array

Yusuke Nagasaki,^{1,2} Behrad Gholipour,^{1,3} Jun-Yu Ou,^{1,a)} Masanori Tsuruta,^{1,4} Eric Plum,¹ Kevin F. MacDonald,¹ Junichi Takahara,^{2,5} and Nikolay I. Zheludev^{1,6}

¹Optoelectronics Research Centre and Centre for Photonic Metamaterials, University of Southampton, Highfield, Southampton SO17 1BJ, United Kingdom

²Graduate School of Engineering, Osaka University, 2-1 Yamadaoka, Suita, Osaka 565-0871, Japan

³Department of Chemistry, University of Southampton, Highfield, Southampton SO17 1BJ, United Kingdom

⁴Asahi Kasei, Energy and Environment R&D Center, 2-1 Samejima, 416-8501 Fuji, Japan

⁵Photonics Advanced Research Center, Osaka University, 2-1 Yamadaoka, Suita, Osaka 565-0871, Japan

⁶Centre for Disruptive Photonic Technologies, SPMS, TPI, Nanyang Technological University, Singapore 637371, Singapore

(Received 9 February 2018; accepted 8 June 2018; published online 13 July 2018)

Non-volatile temperature-induced structural phase transitions such as those found in chalcogenide glasses are known to lead to strong changes in optical properties and are widely used in rewritable optical disk technology. Herein, we demonstrate that thermally activated optical memory can be achieved via the nanostructural reconfiguration of a metallic nanowire metamaterial array made from a shape-memory alloy: A nickel-titanium film of nanoscale thickness structured on the subwavelength scale exhibits bistability of its optical properties upon temperature cycling between 30 °C and 210 °C. The structure, comprising an array of NiTi nanowires coated with a thin film of gold to enhance its plasmonic properties, can exist in two non-volatile states presenting an optical reflectivity differential of 12% via nanoscale mutual displacements of alternating nanowires in the structure. Such all-metal shape-memory photonic gratings and metamaterials may find applications in bistable optical devices. *Published by AIP Publishing.* <https://doi.org/10.1063/1.5025400>

Structuring of materials on length scales comparable to or smaller than the wavelength of electromagnetic radiation enables the design of metamaterials, photonic crystals and gratings with engineered or enhanced optical properties, including properties that are not available in natural materials.^{1,2} Periodically structured surfaces may be referred to as metamaterials or metasurfaces when they interact with radiation that has a wavelength longer than the said period. In respect of shorter wavelengths of radiation, the same structures function as diffractive gratings. Several approaches for tuning, modulating and switching the functionalities of such structured materials have emerged, including (i) mechanical actuation of the internal structure of metamaterials,^{3–9} (ii) inclusion of phase-change media (e.g., chalcogenide glasses, vanadium dioxide, gallium)^{10–12} or nonlinear materials,¹³ and (iii) all-optical “coherent control” of the interaction of ultrathin metamaterials with light.¹⁴ Here, we introduce a reconfigurable photonic nanostructure which exhibits optical memory behaviour underpinned by the shape-memory effect. Shape-memory alloys are binary or ternary metallic alloys that exhibit thermally induced reversible transitions between structural phases with different mechanical properties. Temperature-activated shape-memory effects were first observed in gold-cadmium alloys^{15,16} and became widely used with the discovery of nickel-titanium alloys,^{17,18} leading to a variety of applications ranging from actuators and valves to stents.^{19,20}

To demonstrate thermally activated optical memory with a shape-memory alloy, we developed a device structure,

in which an array of nickel-titanium (NiTi) nanowires supported on silicon nitride nano-beams is covered with a gold layer of nanoscale thickness (Fig. 1). The purpose of the plasmonic gold layer is to enhance the resonant optical characteristics of the nanostructure, while the SiN–NiTi bimorph provides for the hysteretic temperature-activated reconfiguration of the nanostructure that leads to non-volatile changes in the composite’s optical properties. The NiTi alloy was chosen as the active medium because it retains shape-memory properties on the nanoscale.^{21,22} The beams of the

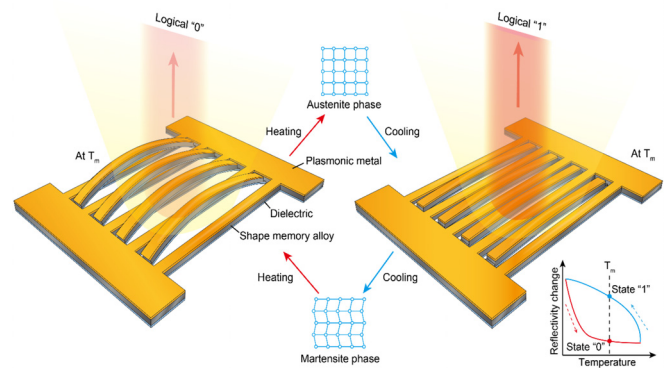


FIG. 1. A shape-memory photonic nanostructure. For a given temperature T_m , the nanostructure has two different stable shapes as shown, depending on the phase of the NiTi alloy component forming the nanostructural framework. Transition between these shapes can be achieved in a temperature cycle within which NiTi transforms between its martensite and austenite phases in a hysteretic fashion. The change in the shape of the nanostructure leads to a change in its plasmonic response and thereby its optical properties, which are dominated by the gold coating on the NiTi framework. (Note that in these artistic sketches, the structural deformation is highly exaggerated and in fact happens at a level comparable to or smaller than the thickness of the nanowires.)

^{a)} Author to whom correspondence should be addressed: jo2c09@orc.soton.ac.uk

array are anchored to the unstructured part of the membrane and every second beam of the array has trenches cut through the gold into the NiTi layer at either end close to the anchor points (see inset to Fig. 2). Temperature variations cause stress in the beams due to differential expansion of the constituent layers. The stress causes a larger deformation of weakly anchored beams (with trench cuts) than strongly anchored beams (without). As the optical properties of the array are sensitive to the mutual positions of the beams, a change in temperature leads to a change in the array's optical properties. The central NiTi shape-memory alloy layer of the structure undergoes a hysteretic transition between martensite and austenite solid phases upon temperature cycling. This leads to a hysteresis in the thermal expansion that drives beam deformation, in turn, giving rise to hysteretic changes in the optical properties of the array.

The shape-memory nanowire array was manufactured on a silicon nitride (SiN) membrane by sputtering of the NiTi alloy, thermal evaporation of gold and subsequent nanostructural patterning by focused ion beam milling. 175 nm of NiTi (42% Ni, 58% Ti) was deposited on a commercially sourced SiN membrane of 50 nm thickness by radio-frequency sputtering (Kurt J. Lesker Nano 38) from 99.999% purity NiTi and Ni targets (Testbourne), providing for accurate control over the deposited film's composition.^{22–24} A base pressure of 4.0×10^{-5} mbar was achieved before deposition. A flow rate of 10 cubic centimetres per minute (SCCM) of high purity argon was used to strike the plasma on both targets. The substrate was held on a rotating platen with a target-substrate distance of approximately 150 mm, which ensures the deposition of low stress films. A working pressure of 2×10^{-3} mbar was achieved during deposition. The sputtering rate was fixed at 3.50 nm/min. The deposited film was subsequently annealed (Jipelec rapid thermal annealer) at 400 °C for 30 min in argon at atmospheric pressure^{24,25} with heating and cooling rates of 50 °C/min and 1 °C/min, respectively (the annealing chamber having first been purged with Ar for 2.5 h to remove air). The final composition of the shape-memory alloy film was determined, by energy-dispersive X-ray spectroscopy, to be 42%

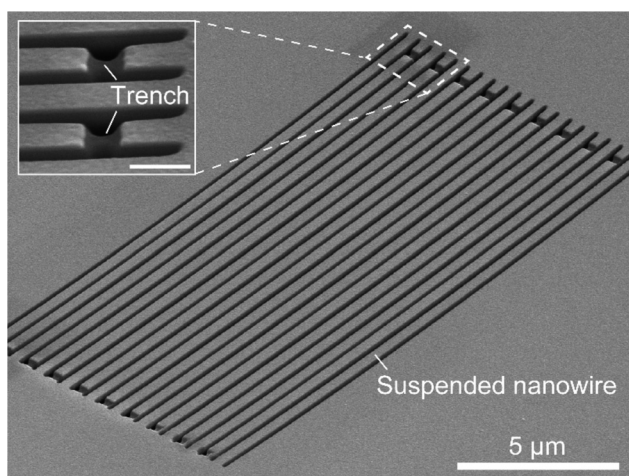


FIG. 2. A shape-memory photonic nanowire metamaterial array. Scanning electron microscopy image of the nanostructure fabricated on a Au-NiTi-SiN nano-membrane. The inset shows the trenches fabricated at the ends of every other beam (scale bar = 500 nm).

Ni and 58% Ti. The 50-nm-thick gold layer was deposited on top of the shape-memory alloy by resistance evaporation (Edwards Auto 306) with a base chamber pressure of 2.0×10^{-6} mbar at a deposition rate of 0.05 nm/s. The nanowire pattern was manufactured by focused ion beam milling (FEI Helios NanoLab 600), cutting through the layers to produce an array of 400-nm-wide freestanding suspended beams separated by 100-nm-wide gaps (Fig. 2). In order to avoid over-milling the gold layer, the nanowires were first milled from the SiN membrane side. Then, the sample was turned over and the trenches were milled from the gold side, to a depth of 150 nm, at both ends of every other beam, as shown in the inset to Fig. 2.

In order to confirm the reversible martensite-austenite transitional behavior of NiTi,²¹ the temperature dependence of resistance of a 175-nm-thick NiTi control sample deposited on a SiO₂ substrate was measured. A 4-probe measurement (Keithley 2636B Sourcemeter) was performed under vacuum at a pressure of 4.0×10^{-6} mbar to prevent sample oxidation. The probes were fixed to the sample with conductive adhesive to prevent separation during temperature cycling, which may otherwise occur due to differential thermal expansion of the sample substrate and probes. Upon temperature cycling between ~ 30 °C and 220 °C, the resistance shows a clear hysteresis loop, which is a characteristic feature of the martensite-to-austenite phase transition for this alloy (Fig. 3). This behaviour is maintained through repeated temperature cycling (tested here up to 7 heating-cooling cycles).

To demonstrate the hysteretic behaviour of the shape memory plasmonic nanostructure's optical properties, reflection spectra were recorded at various points in the heating/cooling temperature cycle using a microspectrophotometer (CRAIC QDI2010) with a 15 \times objective (numerical aperture 0.28). The nanowire structure was illuminated with light linearly polarized perpendicular to the nanowires. Spectra were recorded with an aperture size of $5 \mu\text{m} \times 5 \mu\text{m}$ (i.e., smaller than the $25 \mu\text{m} \times 9.5 \mu\text{m}$ size of the array).

In the absence of deformation, the structure is a metamaterial for wavelengths longer than 500 nm. However, as the differential displacement of every second nanowire doubles the period to 1000 nm, the structure becomes diffracting over

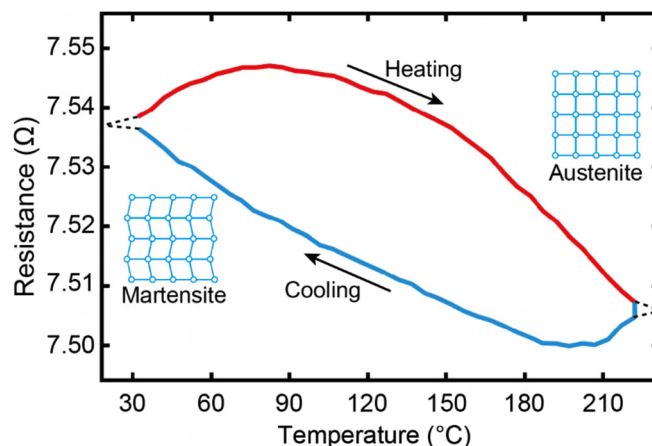


FIG. 3. Hysteretic dependence of resistance on temperature for a 175-nm-thick NiTi film on a fused silica (SiO₂) substrate.

the experimental wavelength range (500 nm–870 nm). In reflective measurements, both illumination of the sample and collection of reflected light occur through an objective with a numerical aperture of 0.28—giving a maximum angle of incidence for illumination and detection of light equal to 16° . As such, the microspectrophotometer does not detect diffracted light from a grating of 1000 nm period at wavelengths greater than 560 nm.

The reflectivity spectrum of the nanostructure shows a local maximum at ~ 500 nm [Fig. 4(a) inset] corresponding to the lattice mode associated with the nanowire spacing. The increase in reflectivity towards the long wavelength end (870 nm) of the measurable spectral range suggests the presence of another reflectivity maximum at longer wavelengths, which may be the lattice mode associated with the 1000 nm spacing of identical nanowires.

To measure the temperature dependence of the nanostructure's reflection properties, it was mounted on a thermostatic sample stage. The stage temperature was varied from 30 to 210°C in 20°C steps, allowing 5 min for the system to reach thermal equilibrium at each temperature. The optical properties of the shape-memory nanowire array are found to be strongly temperature-dependent and hysteretic, which is to say that the nanostructure presents different reflection spectra depending on whether it has been heated or cooled to a given temperature.

Figure 4(a) shows the differential reflectivity spectra of the nanowire array after heating (red) and cooling (blue) to a temperature of 110°C , relative to the reflectivity at a reference temperature of 210°C . Figure 4(b) shows the hysteretic temperature-dependence of reflection at a given wavelength (835 nm). The shape-memory nanowire structure is up to 12% more reflective after cooling to a stage temperature of 110°C (a state that may be denoted logical “1”) as compared to having been heated to the same temperature (logical “0”). Starting at room temperature, the decrease in reflectivity with increasing temperature is consistent with increasing deformation of the nanostructure causing more light to be diffracted. This trend is reversed as the sample is heated above 110°C , implying a gradual phase transition in the NiTi layer. As the nanostructure is cooled, its reflectivity at 835 nm is higher (implying reduced diffraction due to reduced nanowire deformation) than at the same temperature during the heating process, until the reflectivity returns to its original value close to room temperature, indicating that the nanowires have returned to their original state.

We conclude that the observed temperature hysteresis (memory) of optical properties is related to the martensite-austenite cycle in NiTi, which results in the existence of two different stable shapes for the nanostructure. Indeed, finite element analysis (COMSOL Multiphysics) indicates that the midpoint of a nanowire with trenches on either end is displaced out of plane by 105 nm at 110°C when NiTi is in the martensite phase and by 70 nm at the same temperature in the austenite phase [Fig. 4(c)], while the displacement of nanowires without trenches is negligible (<5 nm) for both NiTi phases. The simulations assume flat nanowires at room temperature, with nanowire ends at a fixed position and a fixed orientation, and martensite and austenite phases with thermal expansion coefficients of 7×10^{-6} and $11 \times 10^{-6} \text{K}^{-1}$ (Ref. 26), Young's

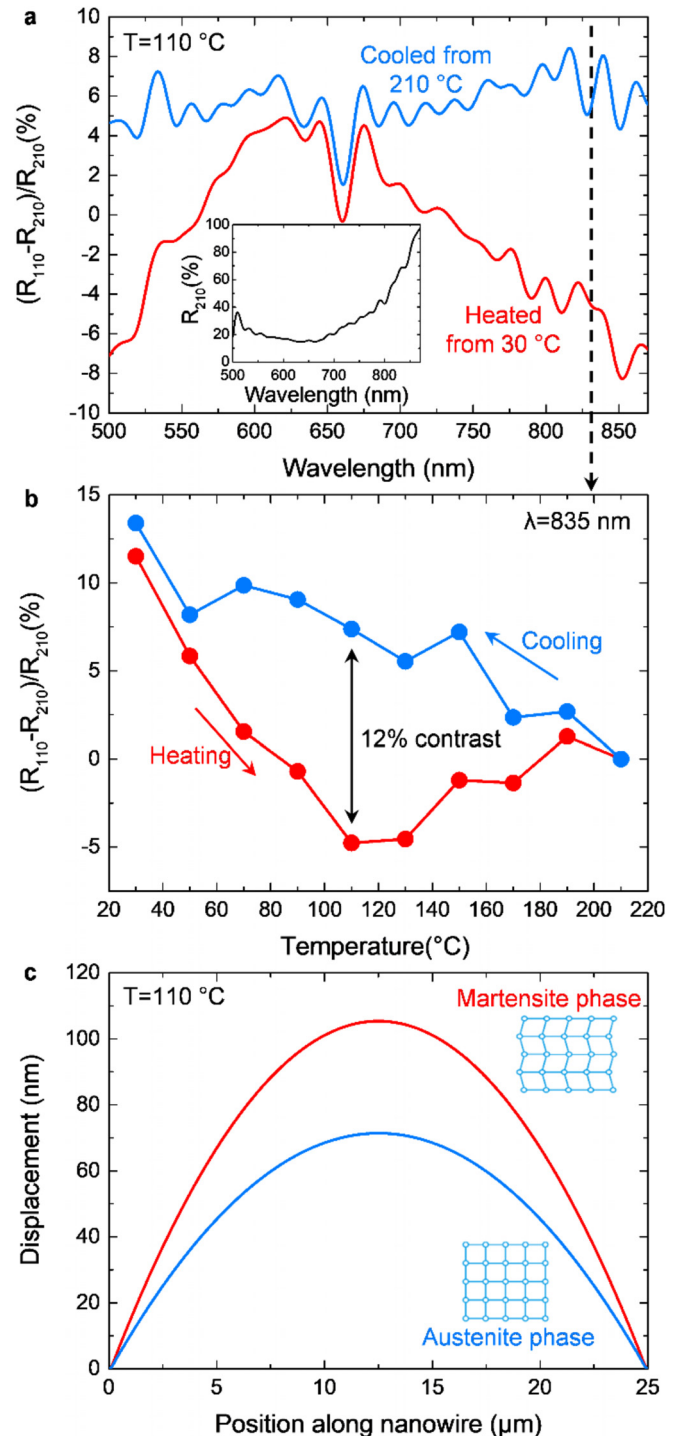


FIG. 4. Deformation-dependent optical properties of the shape-memory nanowire array. (a) Spectral dispersion of the difference between reflectivities of the nanostructure measured at 110°C and 210°C , relative to the reflectivity at 210°C . Blue and red curves correspond to the cooling and heating parts of the hysteresis cycle, respectively. The inset shows the reference reflectivity spectrum at 210°C . (b) Difference between the sample reflectivity at temperatures T and 210°C relative to the reflectivity level at 210°C at a wavelength of 835 nm. (c) Simulated out-of-plane deformation profile of a nanowire with trench cuts at each end for NiTi in the martensite (red) and austenite (blue) states at a temperature of 110°C .

moduli of 28 and 83 GPa, and Poisson's ratio of 0.33 (Ref. 22). As illustrated schematically in Fig. 1, the change in the shape of the nanostructure leads to a change in its plasmonic response and thus in its optical properties, which are dominated by the gold coating on the NiTi framework. An additional contribution

to the change in the nanostructure's optical response may come from a temperature-dependent change in the optical properties of NiTi.

The shape-memory nanowire array reported here demonstrates how non-volatile memory characteristics can be achieved in reconfigurable metamaterial nanostructures based on bimaterial bridge actuators.^{6–9} More generally, shape-memory materials provide a broad range of opportunities for active/adaptive plasmonic devices, metamaterials, gratings and photonic crystals: For example, shape-memory materials could be used to add hysteretic switching and memory functionalities to thermally actuated metamaterials,^{6,8,27,28} which are typically deformed only by differential thermal expansion of different materials rather than phase transitions. Two-way shape-memory alloys¹⁹ could enable pronounced thermal switching of photonic structures between two distinct states, even without relying on differential thermal expansion. This could allow the realization of thermally switchable, bistable magnetic metamaterials based on three-dimensional split ring resonators.^{27–29} Shape-memory polymers, offering reversible strains of up to 800%³⁰ and multi-shape memory,³¹ could act as elastic shape-memory substrates for gratings, photonic crystals and metamaterials reconfigured by stretching.⁵ Furthermore, shape-memory polymers, loaded with nanoparticles to achieve a high refractive index, could even serve as nanoimprint substrates, where imprint in regimes of elastic and plastic deformation³² could be exploited to create temporary and permanent bas-relief metamaterials and gratings,³³ allowing thermal recovery of the latter.

Our proof-of-principle demonstration highlights the opportunity that shape-memory materials provide for reconfigurable photonic nanostructures. The engineering of optimized devices will require systematic studies to achieve an optimal performance of alloy and nanostructures and investigations of device behaviour over a large number of temperature cycles.

In summary, we demonstrate a shape-memory-alloy-based nanomechanical reconfigurable grating. By introducing a phase-change material into a mechanically reconfigurable nanowire array, we realize a mechanically reconfigurable photonic nanostructure with rewritable memory functionality. We believe that shape-memory photonic nanostructures and metamaterials can enable a variety of advanced optical functionalities: In principle, they can be programmed by permanent deformation into complex shapes, tuned by reversible actuation under the influence of thermal, electrical, magnetic or optical control signals, and reset with heat.

The authors are grateful to João Valente for fruitful discussions. This work was supported by Asahi Kasei, the UK's Engineering and Physical Sciences Research Council (Grant Nos. EP/M009122/1 and EP/N00762X/1), the UK's Defence Science and Technology Laboratory (Grant No. DSTLX1000064081), and the Ministry of Education Singapore (Grant No. MOE2016-T3-1-006). Y.N. was supported by Research Fellowships of the Japan Society for

the Promotion of Science (JSPS) for Young Scientists and the Interactive Materials Science Cadet Program of Osaka University and by the JSPS Core-to-Core Program, A. Advanced Research Networks. Following a period of embargo, the data from this paper can be obtained from the University of Southampton ePrints research repository: <https://doi.org/10.5258/SOTON/D0557>.

- ¹N. I. Zheludev, *Science* **348**, 973–974 (2015).
- ²A. F. Koenderink, A. Alù, and A. Polman, *Science* **348**, 516–521 (2015).
- ³M. Lapine, D. Powell, M. Gorkunov, I. Shadrivov, R. Marqués, and Y. Kivshar, *Appl. Phys. Lett.* **95**, 084105 (2009).
- ⁴H. Tao, A. C. Strikwerda, K. Fan, W. J. Padilla, X. Zhang, and R. D. Averitt, *Phys. Rev. Lett.* **103**, 147401 (2009).
- ⁵I. M. Pryce, K. Aydin, Y. A. Kelaita, R. M. Briggs, and H. A. Atwater, *Nano Lett.* **10**, 4222–4227 (2010).
- ⁶J. Y. Ou, E. Plum, L. Jiang, and N. I. Zheludev, *Nano Lett.* **11**, 2142–2144 (2011).
- ⁷J.-Y. Ou, E. Plum, J. Zhang, and N. I. Zheludev, *Nat. Nanotechnol.* **8**, 252–255 (2013).
- ⁸J. Valente, J.-Y. Ou, E. Plum, I. J. Youngs, and N. I. Zheludev, *Appl. Phys. Lett.* **106**, 111905 (2015).
- ⁹N. I. Zheludev and E. Plum, *Nat. Nanotechnol.* **11**, 16–22 (2016).
- ¹⁰T. Driscoll, H.-T. Kim, B.-G. Chae, B.-J. Kim, Y.-W. Lee, N. M. Jokerst, S. Palit, D. R. Smith, M. D. Ventra, and D. N. Basov, *Science* **325**, 1518–1521 (2009).
- ¹¹B. Gholipour, J. Zhang, K. F. MacDonald, D. W. Hewak, and N. I. Zheludev, *Adv. Mater.* **25**, 3050–3054 (2013).
- ¹²R. F. Waters, P. A. Hobson, K. F. MacDonald, and N. I. Zheludev, *Appl. Phys. Lett.* **107**, 081102 (2015).
- ¹³M. Lapine, I. V. Shadrivov, and Y. S. Kivshar, *Rev. Mod. Phys.* **86**, 1093–1123 (2014).
- ¹⁴J. Zhang, K. F. MacDonald, and N. I. Zheludev, *Light Sci. Appl.* **1**, e18 (2012).
- ¹⁵G. V. Kurdyumov and L. G. Khandros, *Dokl. Akad. Nauk SSSR* **66**, 211–214 (1949).
- ¹⁶L. C. Chang and T. A. Read, *Trans. AIME* **189**, 47–52 (1951).
- ¹⁷W. J. Buehler, J. V. Gilfrich, and R. C. Wiley, *J. Appl. Phys.* **34**, 1475–1477 (1963).
- ¹⁸K. Otsuka and X. Ren, *Prog. Mater. Sci.* **50**, 511–678 (2005).
- ¹⁹K. Otsuka and C. M. Wayman, *Shape Memory Materials* (Cambridge University Press, 1999).
- ²⁰J. M. Jani, M. Leary, A. Subic, and M. A. Gibson, *Mater. Des.* **56**, 1078–1113 (2014).
- ²¹*Thin Film Shape Memory Alloys: Fundamentals and Device Applications*, edited by S. Miyazaki, Y. Q. Fu, and W. M. Huang (Cambridge University Press, 2009).
- ²²Y. Q. Fu, S. Zhang, M. J. Wu, W. M. Huang, H. J. Du, J. K. Luo, A. J. Flewitt, and W. I. Milne, *Thin Solid Films* **515**, 80–86 (2006).
- ²³A. Ishida, A. Takei, and S. Miyazaki, *Thin Solid Films* **228**, 210–214 (1993).
- ²⁴P. Surlbled, C. Clerc, B. L. Pioufle, M. Ataka, and H. Fujita, *Thin Solid Films* **401**, 52–59 (2001).
- ²⁵J.-L. Seguin, M. Bendahan, A. Isalgue, V. Esteve-Cano, H. Carchano, and V. Torra, *Sens. Actuators A* **74**, 65–69 (1999).
- ²⁶J. Uchil, K. P. Mohanchandra, K. G. Kumara, K. K. Mahesh, and T. P. Murali, *Physica B* **270**, 289–297 (1999).
- ²⁷C. C. Chen, C. T. Hsiao, S. Sun, K.-Y. Yang, P. C. Wu, W. T. Chen, Y. H. Tang, Y.-F. Chau, E. Plum, G.-Y. Guo, N. I. Zheludev, and D. P. Tsai, *Opt. Exp.* **20**, 9415–9420 (2012).
- ²⁸Y. Mao, Y. Pan, W. Zhang, R. Zhu, J. Xu, and W. Wu, *Nano Lett.* **16**, 7025–7029 (2016).
- ²⁹C.-C. Chen, A. Ishikawa, Y.-H. Tang, M.-H. Shiao, D. P. Tsai, and T. Tanaka, *Adv. Opt. Mater.* **3**, 44–48 (2015).
- ³⁰W. Voit, T. Ware, R. R. Dasari, P. Smith, L. Danz, D. Simon, S. Barlow, S. R. Marder, and K. Gall, *Adv. Funct. Mater.* **20**, 162–172 (2010).
- ³¹T. Pretsch, *Smart Mater. Struct.* **19**, 015006 (2010).
- ³²Q. Zhao, W. Zou, Y. Luo, and T. Xie, *Sci. Adv.* **2**, e1501297 (2016).
- ³³J. Zhang, J.-Y. Ou, K. F. MacDonald, and N. I. Zheludev, *J. Opt.* **14**, 114002 (2012).